Performance of Seismic Design Aids for Nonlinear Pushover Analysis of Reinforced Concrete and Steel Bridges

Franklin Y. Cheng & Jeffrey Ger
Missouri University of Science and Technology, Rolla, Missouri, USA

SUMMARY:
Nonlinear static monotonic (pushover) analysis has become a common practice in performance-based bridge seismic design. The popularity of pushover analysis is due to its ability to identify the failure modes and the design limit states of bridge piers and to provide the progressive collapse sequence of damaged bridges when subjected to major earthquakes. Unfortunately, there is no complete technical reference in this field to provide the practicing engineer step-by-step procedures for pushover analyses and various nonlinear member stiffness formulations. This paper provides an overview of a newly published book "Seismic Design Aids for Nonlinear Pushover Analysis of Reinforced Concrete and Steel Bridges**"** by the authors of this paper, which fills the need for a complete reference on pushover analysis for practicing engineers. This technical reference provides five different nonlinear element stiffness formulation methods, ranging from the simplest to the most sophisticated, suitable for engineers at various levels of nonlinear structural analysis experience. The authors also provide a downloadable computer program, INSTRUCT (INelastic STRUCTural Analysis of Reinforced-Concrete and Steel Structures), that allows readers to perform their own pushover analyses. Several real-world examples provided in this paper demonstrate the accuracy of INSTRUCT's analytical prediction by comparing numerical results with full- or large-scale test results, and excellent performance by INSTRUCT is observed.

Keywords: Pushover, Seismic, Plastic hinge, failure modes, bridges

1. NONLINEAR PUSHOVER ANALYSIS PROCEDURE

The nonlinear pushover analysis is governed by the following equations.

$$[K]\{\Delta\delta\} = \{\Delta F\} + \{U\} \tag{1.1}$$

Partitioning the structural global stiffness $[K]$, displacement $\{\Delta\delta\}$, load $\{\Delta F\}$, and unbalanced force $\{U\}$ matrices between free, (f), and restrained, (r), degrees of freedom, yields

$$\begin{bmatrix} [K_{ff}] & [K_{fr}] \\ [K_{rf}] & [K_{rr}] \end{bmatrix} \begin{bmatrix} \{\Delta\delta_f\} \\ \{\Delta\delta_r\} \end{bmatrix} = \begin{bmatrix} \{\Delta F_f\} + \{U_f\} \\ \{\Delta R\} + \{U_r\} \end{bmatrix} \tag{1.2}$$

where $\{\Delta\delta_r\}$ represents the imposed displacement vector (i.e. displacement control); $\{\Delta R\}$ represents the reaction vector, and $\{\Delta F_f\}$ is the incremental joint load vector (i.e. force control). INSTRUCT can perform both force and displacement controls concurrently during the pushover analysis. Expanding Equation (1.2)

$$[K_{ff}]\{\Delta\delta_f\} + [K_{fr}]\{\Delta\delta_r\} = \{\Delta F_f\} + \{U_f\} \tag{1.3}$$

$$[K_{rf}]\{\Delta\delta_f\} + [K_{rr}]\{\Delta\delta_r\} = \{\Delta R\} + \{U_r\} \tag{1.4}$$

Rewriting Equation (1.3) yields

$$[K_{ff}]\{\Delta\delta_f\} = \{\Delta F_f\} + \{U_f\} - [K_{fr}]\{\Delta\delta_r\} \tag{1.5}$$

which is solved for the free global degrees of freedom $\{\Delta\delta_f\}$ by Gaussian elimination. Rewriting Equation (1.4) yields the reactions

$$\{\Delta R\} = [K_{rf}]\{\Delta\delta_f\} + [K_{rr}]\{\Delta\delta_r\} - \{U_r\} \tag{1.6}$$

The total structural global displacements, forces, and reactions at load step t are determined from

$$\{\delta^t\} = \{\delta^{t-1}\} + \{\Delta\delta^t\};\ \{F^t\} = \{F^{t-1}\} + \{\Delta F^t\};\ \{R^t\} = \{R^{t-1}\} + \{\Delta R^t\} \tag{1.7}$$

Once the total global displacement increment vector, $\{\Delta\delta^t\}$, is obtained, the individual member deformation increment vector, $\{\Delta\delta_e^t\}$, can be calculated by

$$\{\Delta\delta_e^t\} = [A]^T\{\Delta\delta^t\};\ \{\Delta F_e^t\} = [k_e]\{\Delta\delta_e^t\} \tag{1.8}$$

where $[A]^T$ is the transformation matrix between the global displacements increment vector and the member deformation increment vector. $\{\Delta F_e^t\}$ is the element force increment vector at load step t. $[k_e]$ is the individual element stiffness matrix. At the end of load step *t*, the element unbalanced force vector is calculated, as is the difference between the calculated element force vector from Equation (1.8) and the element force vector calculated based on the element's hysteresis model or stress resultants from steel and concrete stress-strain relationships. These member unbalanced forces are transferred to the structural global degrees of freedom to form the global unbalanced joint force vector $\{U\}$ for the next step. At each step, the individual element stiffness matrix is updated according to the element's hysteresis model or material stress-strain relationship.

2. MATERIAL LIBRARY

INSTRUCT provides a material library covering 12 different material models. They are:

1) Elastic 3D Prismatic Beam Material (3D-BEAM).
2) Bilinear Hysteresis Model (BILINEAR): A hysteretic material model that has a bilinear backbone curve and an elastic unloading and reloading curve. This model is mainly used for spring elements described in the element library later.
3) Gap/Restrainer Model (GAP): This hysteresis model simulates the inelastic behavior of restrainer or expansion joints.
4) Takeda Hysteresis Model (TAKEDA): The Takeda model is mainly used to model the bending deformation of reinforced concrete members subjected to cyclic loading.
5) Bilinear Moment-Rotation Model (HINGE): This model is only used in the inelastic 3D-beam (IE3DBEAM) element described in the element library later.
6) Bilinear Hysteresis Model (IA_BILN): This model is used in the IE3DBEAM element. The model has a bilinear bending backbone curve and an elastic unloading and reloading curve.
7) Finite-Segment Steel Stress-Strain Hysteresis Model (STABILITY1): This model can be either a bilinear stress-strain relationship, or a Ramberg-Osgood stress-strain relationship. The model is only used for the finite-segment element described in the element library later.
8) Finite-Segment Reinforced Concrete Stress-Strain Hysteresis Model (R/CONCRETE1): This model is based on Mander's concrete stress-strain relationship (Mander, Priestley, and Park,

1988). It is only used for the finite-segment element.
9) Finite-Segment Moment-Curvature Model (MOMCURVA1): This model is based on user-defined backbone moment-curvature curves, and is only used for the finite-segment element.
10) Plate Material (PLATE): This material defines the elastic material properties for the rectangular plate element.
11) Point Material (POINT): This material defines the elastic material properties for the POINT element.
12) Brace Material (BRACE): This material defines the hysteresis rule of Jain-Goel-Hanson's model (1980). The model is mainly for struts with angle and rectangular tube sections. For I-shape sections, several control points in the model are modified in order to fit the experimental results achieved by Black, Wenger, and Popov (1980).

3. ELEMENT LIBRARY

INSTRUCT provides an element library covering 7 element types. They are:
1) Elastic 3D-Prismatic Element (3D-BEAM): This element has 12 degrees-of-freedom. The element considers axial deformation, torsional deformation, and bending deformations. Warping torsion and shear deformation are not considered. The geometric stiffness for $P-\delta$ effects is available.
2) Spring Element (SPRING): The spring element may behave elastically or nonlinearly depending on the material properties used. The spring could be axial, shear, or rotational spring.
3) Inelastic 3D-Beam Element (IE3DBEAM): This element has 12 degrees-of-freedom. The geometric stiffness for $P-\delta$ effects is available. IA_BILN, HINGE, or TAKEDA material could be used for this element.
4) Finite-Segment Element (STABILITY): the member (see Figure 4.5) is divided into several segments. Each segment has 12 degrees of freedom and the cross section is divided into many small elements (or so called strings). The finite-segment element connects a start and an end joint. The element considers nonlinear axial and bending deformations. Warping torsion and shear deformation are not considered. The STABILITY1, R/CONCRETE1, or MOMCURVA1 hysteresis material model described in the previous section can be used for the finite segment element. The second order P-δ forces are considered in the element stiffness matrix formulation.
5) Plate Element (PLATE): The plate element consists of a plate linking four joints, and has 5 degrees-of-freedom at each joint (three translational and 2 rotational).
6) Point Element (POINT): The point element is a point consisting of a 6 x 6 stiffness matrix. For example, bridge foundation stiffnesses can be modeled by point elements.
7) Brace Element (BRACE): Brace Material (BRACE) is used for this element.

4. NONLINEAR BENDING STIFFNESS MATRIX

This section describes how INSTRUCT formulates the nonlinear element bending stiffness matrix using five different methods, 1) Bilinear Interaction Axial Load-Moment (PM), 2) Plastic Hinge Length (PHL), 3) Constant Moment Ratio (CMR), 4) Finite Segment–Finite String (FSFS), and 5) Finite Segment–Moment Curvature (FSMC) methods. The PM, PHL, and CMR methods are simpler than FSFS and FSMC, with FSFS method being the most sophisticated.

4.1. Bilinear Interaction Axial Load -Moment (PM) Method

The bilinear moment-curvature curve shown in Figure 4.1(a) is used to generate the non-linear member bending stiffness matrix. The moment-curvature curve is composed of two imaginary components shown in Figure 4.1(b). In these figures, the slopes of the linear and elasto-plastic

components are $a1 = p \times EI$, $a2 = q \times EI$, and $p + q = 1$, where p is the fraction of flexural rigidity apportioned to the linear component and q is the fraction of flexural rigidity apportioned to the elasto-plastic component. The post-yield slope of the elasto-plastic component is equal to zero.

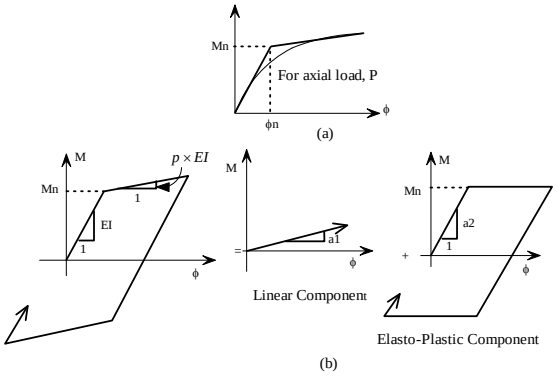

Figure 4.1. Bilinear moment-curvature model

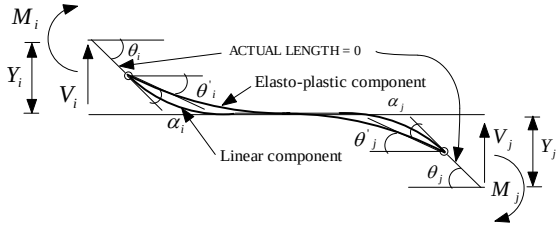

Figure 4.2. Nonlinear member

The nonlinear member shown in Figure 4.2 is used to formulate the nonlinear bending member stiffness matrix. In the figure, θ_i and θ_j are member-end total rotations; α_i and α_j are plastic rotations at each end of the elasto-plastic component. Based on Figures 4.1 and 4.2, the member stiffness matrix at any incremental step can be formulated according to the state of yield. The state of yield may be one of the following four conditions: (a) both ends linear, (b) i end nonlinear and j end linear, (c) i end linear and j end nonlinear, and (d) both ends nonlinear. For the derivation of the member stiffness matrix at different yield states, see reference Ger and Cheng (2011). The actual member stiffness matrix incorporated into the INSTRUCT program is 12×12 , which includes bending, axial, and torsional loads for the Inelastic 3D-Beam (IE3DBEAM) element.

4.2. Plastic Hinge Length (PHL) Method

One of the popular methods used for the nonlinear pushover analysis of bridges with concrete columns is the Plastic Hinge Length (PHL) method. In this method, the stiffness matrix of a column is formulated by the combination of an elastic column element and a non-linear rotational spring connected at each end of the element as shown in Figure 4.3. The stiffness of the rotational spring is governed by the moment-rotational curve of a hinge with length L_p , which is called the plastic hinge length. The empirical equation for L_p is available, and can be calibrated using experimental data from large-scale test concrete columns. The member stiffness matrix can be derived (Ger and Cheng, 2011) using the modified slope-deflection theory.

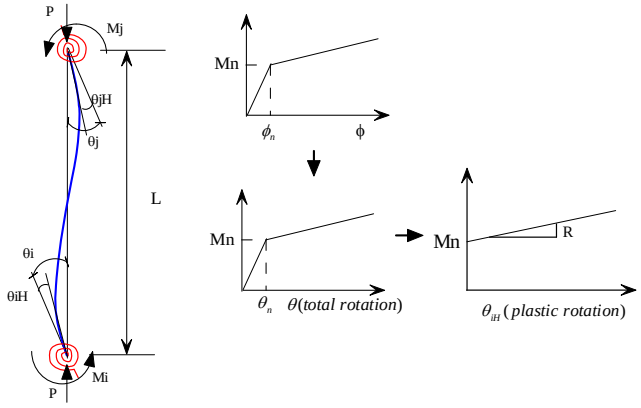

Figure 4.3. Plastic hinge length method

4.3. Constant Moment Ratio (CMR) Method

In the CMR method, the nonlinear bending stiffness matrix is derived based on a simply supported structural model as shown in Figure 4.4. Given a member of length L, the end moments M_i, M_j, and the moment-curvature relationship, the end moment-rotation relationship at each end can be obtained by the conjugate beam theory. The element bending stiffness matrix is obtained by the inversion of the element flexibility matrix which is the superimposition of the elastic element flexibility matrix and the inelastic element flexibility matrix (Ger and Cheng, 2011).

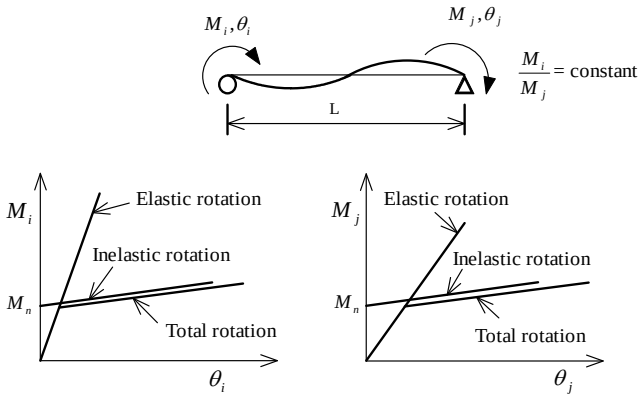

Figure 4.4. Moment-rotation relationship

4.4. Finite Segment-Finite String (FSFS) Method

Another common method of nonlinear pushover analysis is the use of the distributed plasticity model. Using this method, a structural member (for example, a bridge column) is divided into several segments (Chen and Lui, 1991; Chen and Atsuta, 1977). Each segment has 12 degrees-of-freedom and its cross section is divided into many finite elements (or so called finite strings) along the segment's longitudinal direction as shown in Figure 4.5. When a load or displacement increment is applied to a member in the pushover analysis, each segment is deformed and may become partially plastic as sketched in Figure 4.5. The plastification of the cross section can be detected by the steel and concrete stress-strain relationships. For simplicity, the segment's cross sectional plastification and strains are calculated based on the average curvature along the segment length. The member stiffness matrix is established by stacking up the segment stiffness matrix with consideration of the segmental instant location at each incremental step and P-δ effects. For the derivation of the member stiffness matrix, see Ger and Cheng (2011).

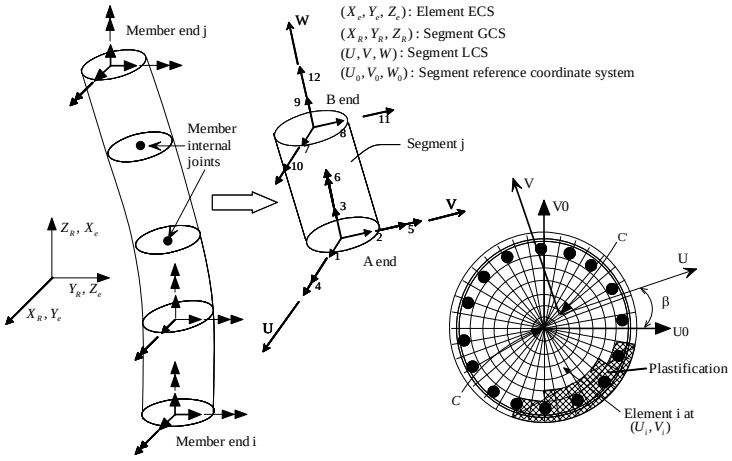

Figure 4.5. Finite segment-sinite string (FSFS) method based on the distributed plasticity model

4.5. Finite Segment-Moment Curvature (FSMC) Method

This method is similar to the FSFS method except that the cross section of each segment is not divided into many elements. The segment stiffness matrix at each incremental step is calculated based on the cross-sectional axial load-moment-curvature family of curves from which the flexural property, EI (i.e. the slope of moment-curvature curve) can be obtained. The total curvature at each step is the accumulation of the incremental curvatures from the previous steps. Similar to the FSFS method, the member stiffness matrix is established by stacking up the segment stiffness matrix with consideration of the segmental instant location and P-δ effects. For the derivation of the member stiffness matrix, see Ger and Cheng (2011).

5. CONCRETE COLUMN FAILURE MODES

Since most bridge columns are reinforced concrete columns, it is necessary to check all the possible concrete column failure modes in the pushover analysis. Possible concrete column failure modes include: 1) Compression failure of unconfined concrete due to the fracture of transverse reinforcement; 2) Compression failure of confined concrete due to the fracture of transverse reinforcement; 3) Compression failure due to buckling of the longitudinal reinforcement; 4) Longitudinal tensile fracture of reinforcing bars; 5) Low cycle fatigue of the longitudinal reinforcement; 6) Failure in the lap-splice zone; 7) Shear failure of the member that limits ductile behavior; 8) Failure of the beam-column connection joint. INSTRUCT is capable of checking all the possible concrete column failure modes. The analytical approaches used to check individual failure modes are also described in Ger and Cheng (2011).

6. CONCRETE COLUMN INTERACTION CURVES

The bilinear moment-curvature curves are used in the PM and PHL methods to formulate the element flexural stiffness matrix. INSTRUCT incorporates not only axial load-nominal moment but also axial load –plastic curvature capacity interactions into the stiffness matrix formulation.

7. PERFORMANCE OF INSTRUCT

Several numerical examples are provided here to examine the performance of INSTRUCT.

Example 1 - Moment-Curvature Analysis: A column cross section and material details from the FHWA Seismic Design Example No. 4 (FHWA, 1996) were used here to generate the moment-curvature curves, where: column diameter =48"; longitudinal reinforcement is 34 - #11; $f_c^{'}$ =4 ksi; f_y =60 ksi; spiral = #5 @3.5"; concrete cover = 2.63" ; and the applied axial load = 660 kips. The post yield modulus of the reinforcing steel stress-strain curve is assumed to be 1% of the elastic modulus. Figure 7.1 shows the comparison of the moment-curvature curves generated by INSTRUCT and by the direct cross-sectional moment-curvature analysis (SEQMC, 1998). It can be seen that the curves are almost identical. Also Figure 7.2 shows a comparison of moment-curvature curves of a $W8\times31$ wide flange section, generated by INSTRUCT and from Chen and Lui (1991). Good agreement is observed.

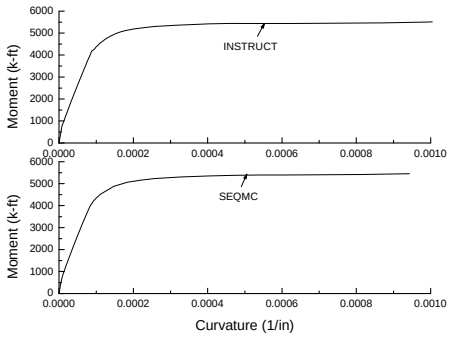

Figure 7.1. Moment-curvature curve comparison

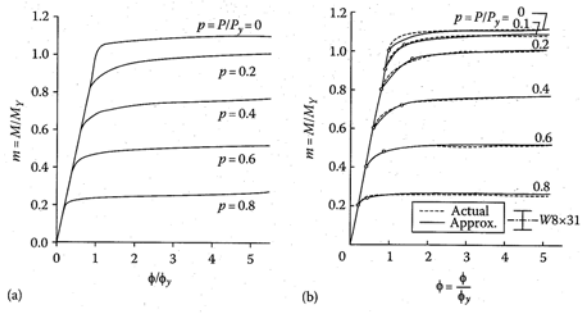

Figure 7.2. Comparison of moment-curvature curves, (a) by INSTRUCT, (b) Chen and Lui (1991)

Example 2 – (a) Column with Rectangular Section: This example compares the numerical results with test results for a column specimen tested at the University of Canterbury, New Zealand (Zahn, Park, Priestley, 1986). The test setup and structural model are shown in Figure 7.3. In Figure 7.4, it can be seen that the lateral force – lateral displacement curve generated by the FSFS method is in agreement with the test results. (b) Column with Circular Section: Figure 7.5 shows the full-scale column test conducted by the National Institute of Standards and Technology (NIST) (Stone and Cheok ,1989). The column is pushed by incremental displacement control at the top of the column. Good agreement is also observed in Figure 7.6.

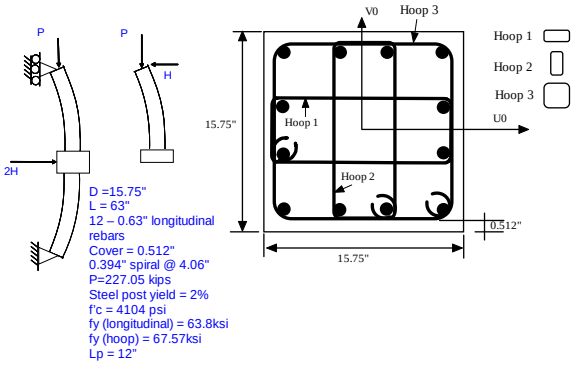

Figure 7.3. Column with rectangular section

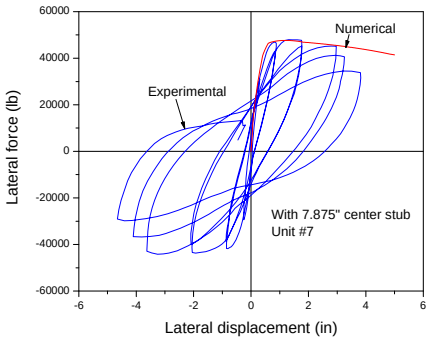

Figure 7.4. Pushover curve comparison

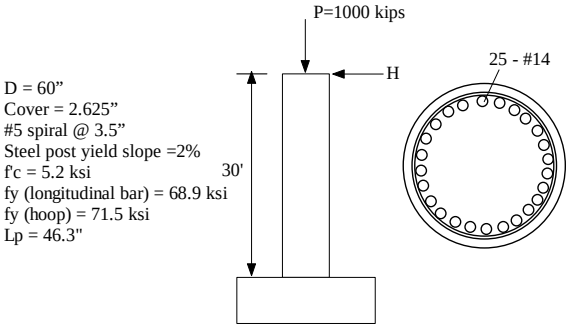

Figure 7.5. NIST 30’ full-scale column

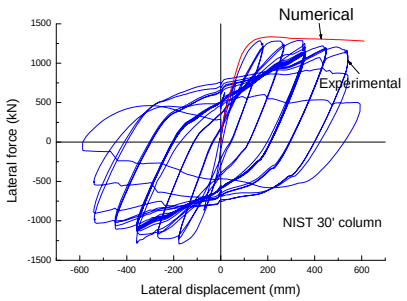

Figure 7.6. Experimental and numerical comparison

Example 3 – Beam-Column Joint Failure: Figure 7.7 shows the full-scale inversed cap beam-column test specimen #1, tested at the University of California, San Diego (Seible, Priestley, Latham, and Silva, 1994). The specimen was post-tensioned. The longitudinal reinforcement consists of 20 - #18 rebars with f_y = 77.5 ksi. The concrete cover is 2 in. The transverse reinforcement is #6 @ 3.5” with f_y = 62.3 ksi. Concrete strength is f'_c = 6 ksi. The IE3DBEAM element with PHL method was used in the analysis. The output from INSTRUCT shows that the joint shear stress reaches the shear stress capacity of 0.548 ksi. The predicted joint shear failure mode is consistent with the UCSD full-scale test result. Figure 7.8 compares the numerical pushover curve with the test results. Good agreement is observed.

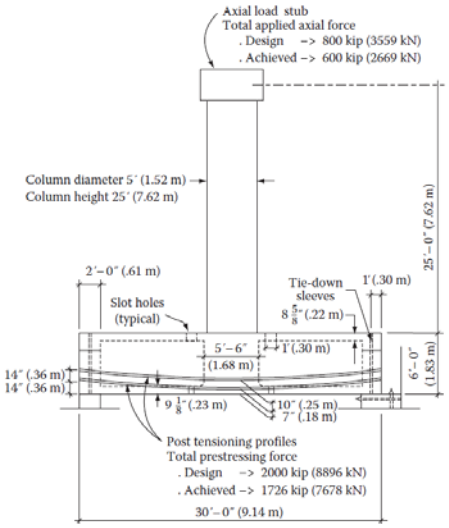

Figure 7.7. Test specimen #1 (copied from Ref. Seible, Priestley, Latham, and Silva, 1994)

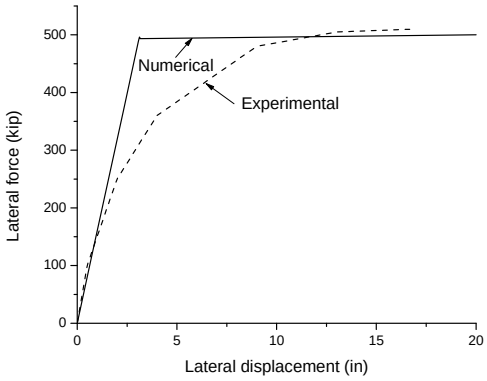

Figure 7.8. Pushover curve for test specimen #1

Example 4 – Four Column Bent: A four-column intermediate bent with circular R/C columns is shown in Figure 7.9. Five P/S I-girders are placed on the cap beam. The cross-sectional properties of the columns are: diameter = 32”; cross-sectional area = 804.25 (in^2); f'_c =4000 psi; E_c =3,605,000 psi; G = 1,442,000 psi; longitudinal bars = 18 - #11; spiral bar = #5 @ 3” pitch; f_y =60 ksi; E_s =29,000 ksi; and plastic hinge length = 25”. The superstructural center of the mass is 78” above the centerline of the cap beam. The cap beam is 42” deep and 42” wide, and assumed to be elastic. The FSFS method is used to find the displacement capacity of the bent by applying pushover displacement at the “master”

joint 11 (i.e. at the superstructural mass center) in the Global Coordinate System (GCS) X direction. Joints 6, 7, 8, and 9 are "slave" joints and constrained by the "master" joint. The lateral displacement capacity is determined when the first column confined concrete strain in the cross-sectional compression region reaches the ultimate concrete compression strain, ε_{cu}, defined as $\varepsilon_{cu} = 0.004 + (1.4\rho_s f_{yh}\varepsilon_{su} / f_{cc}^{'})$ (Priestley, Seible and Calvi, 1996) , where ρ_s is the volumetric ratio of transverse steel; ε_{su} is the ultimate strain of transverse steel (ε_{su} =0.09); f_{yh} is yield stress of transverse steel; and $f_{cc}^{'}$ is the confined concrete strength. The output result shows that the displacement capacity of the bent is reached at pushover displacement of 11.88 inches at which the confined concrete compression strain of member 4 reaches its ε_{cu} of 0.021 (Figure 7.10).

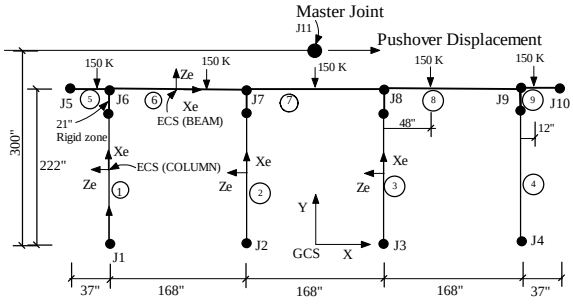

Figure 7.9. Four-column bent

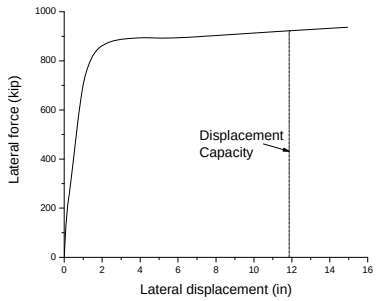

Figure 7.10. Pushover curve at master joint 11

Example 5 – Pile Cap Bent: A pile-cap intermediate bent shown in Figure 7.11 contains four steel HP piles, diagonal angle braces and horizontal braces. The axial load-moment interaction of the steel pile is considered in the pushover analysis. The steel members have yield stress of 36 ksi. The post-buckling of brace members is considered in the analysis. The stiffnesses of the pile-soil interaction are modeled using POINT elements for each pile. The structural model is shown in Figure 7.12. The performance-based criteria for this example are as follows: Pile plastic rotation capacity, θ_p , is 0.05 rad. The maximum allowable brace tensile elongation is assumed to be 10 times that of the brace yield elongation. Find the displacement capacity of the bent by applying incremental pushover displacement at joint 5 in the GCS's X direction. The output results indicate that the brace element No. 20 buckled first (see Figure 7.14) with corresponding pushover displacement = 0.52 in. The displacement capacity of the bent is reached at pushover displacement = 6.6 inches at which the elongation of brace element No. 22 exceeds the allowable elongation of 1.27 inches (Figure 7.13).

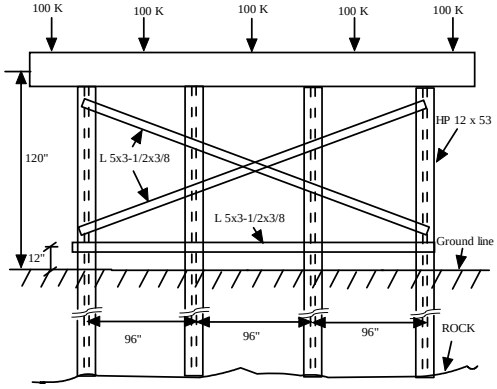

Figure 7.11. Pile-cap bent

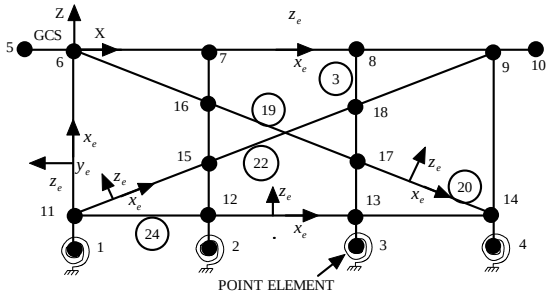

Figure 7.12. Pile-cap bent structural model

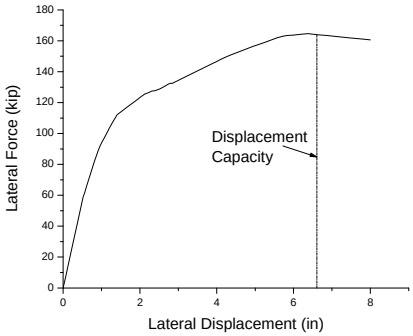

Figure 7.13. Pushover curve at joint 5

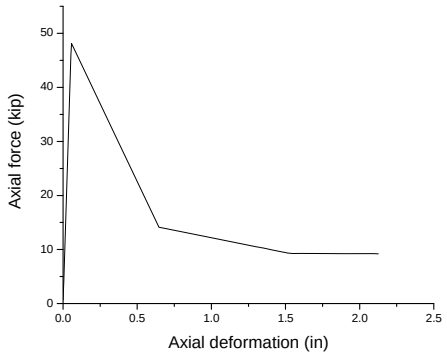

Figure 7.14. Post-buckling of brace element 20

8. CONCLUSION

This paper provides an overview of a new published book "Seismic Design Aids for Nonlinear Pushover Analysis of Reinforced Concrete and Steel Bridges**"** by the authors, which provides step-by-step procedures for pushover analysis with various nonlinear member stiffness formulations ranging from the simplest to the most sophisticated suitable for engineers with varying levels of experience in nonlinear structural analysis. The authors also provide a downloadable computer program, INSTRUCT, that allows readers to perform their own pushover analyses. INSTRUCT checks all the possible concrete column failure modes in the pushover analysis. Numerous real-world examples demonstrate the accuracy of analytical prediction by comparing numerical results with full- or large-scale test results. A useful reference for researchers and engineers working in structural engineering, this book also offers an organized collection of nonlinear pushover analysis applications for students.

REFERENCES

Black, R.G., Wenger, W.A.B., and Popov, E.P. (1980). Inelastic buckling of steel structures under cyclic load reversals, *EERC*, University of California-Berkeley, CA, **Report No.** UCB/EERC-80140.

Chen, W.F. and Atsuta, T. (1977). Theory of Beam-Columns, McGraw-Hill Book Co., New York, **Vol. 2**, 504-527.

Chen, W.F. and Lui, E.M. (1991). Stability Design of Steel Frames, CRC Press, Inc.

Federal Highway Administration. (1996). Seismic Design of Bridges, Design Example No. 4, FHWA-SA-97-009.

Ger, J. And Cheng, F. (2011). Seismic Design Aids for Nonlinear Pushover Analysis of Reinforced Concrete and Steel Bridges, CRC Press, Taylor & Francis Group.

Jain, A.K., Goel, S.C., and Hanson, R.D. (1980). Hysteretic cycles of axially loaded steel members. *Journal of the Structural Division, ASCE*, **Vol 106**, 1777-1795.

Mander, J.B., Priestley, J.N., and Park, R. (1988). Theoretical stress-strain model for confined concrete. *Journal of Structural Engineering, ASCE*, **Vol 114(8),** 1804-1826.

Priestley, J.N., Seible, F., and Calvi, G.M. (1996). Seismic Design and Retrofit of Bridges, Wiley, New York.

SEQMC, Demo version 1.00.06. (1998). Moment-curvature analysis package for symmetric sections.

Seible, F., Priestley, N., Latham, C., and Silva, P. (1994). Full-scale bridge column/superstructure connection tests under simulated longitudinal seismic loads. **Report No.** SSRP-94/14, University of California, San Diego.

Stone, W.C. and Cheok, G.S. (1989). Inelastic behaviour of full-scale bridge columns subjected to cyclic loading. NIST Building Science **Series No.** 166.

Zahn, F.A., Park, R., and Priestley, M.J.N. (1986). Design of reinforced concrete bridge columns for strength and ductility, **Report No.** 86-7, Department of Civil Engineering, University of Canterbury, Christchurch, New Zealand.